

Cross-validation based adaptive sampling for Gaussian process models

Hossein Mohammadi ^{*1, 2}, Peter Challenor^{1, 2}, Daniel Williamson¹, and Marc Goodfellow^{1, 2}

¹College of Engineering, Mathematics and Physical Sciences, University of Exeter, Exeter, UK

²EPSRC Centre for Predictive Modelling in Healthcare, University of Exeter, Exeter, UK

Abstract

In many real-world applications, we are interested in approximating black-box, costly functions as accurately as possible with the smallest number of function evaluations. A complex computer code is an example of such a function. In this work, a Gaussian process (GP) emulator is used to approximate the output of complex computer code. We consider the problem of extending an initial experiment (set of model runs) sequentially to improve the emulator. A sequential sampling approach based on leave-one-out (LOO) cross-validation is proposed that can be easily extended to a batch mode. This is a desirable property since it saves the user time when parallel computing is available. After fitting a GP to training data points, the expected squared LOO error (ESE_{LOO}) is calculated at each design point. ESE_{LOO} is used as a measure to identify important data points. More precisely, when this quantity is large at a point it means that the quality of prediction depends a great deal on that point and adding more samples in the nearby region could improve the accuracy of the GP model. As a result, it is reasonable to select the next sample where ESE_{LOO} is maximum. However, such quantity is only known at the experimental design and needs to be estimated at unobserved points. To do this, a second GP is fitted to the ESE_{LOO} s and where the maximum of the modified expected improvement (EI) criterion occurs is chosen as the next sample. EI is a popular acquisition function in Bayesian optimisation and is used to trade-off between local/global search. However, it has tendency towards exploitation, meaning that its maximum is close to the (current) “best” sample. To avoid clustering, a modified version of EI, called pseudo expected improvement, is employed which is more explorative than EI and allows us to discover unexplored regions. The results show that the proposed sampling method is promising.

*Corresponding Author: h.mohammadi@exeter.ac.uk

Keywords: Adaptive sampling; Computer experiment; Leave-one-out cross-validation; Gaussian processes

1 Introduction

In many real-world applications, we are interested in predicting the output of complex computer codes (or simulators) by cheap-to-evaluate surrogate models, also called emulators. For example, high-fidelity numerical solvers such as computational fluid dynamics and finite element method are computationally intensive and they cannot be used in analysis that requires very many runs. In this situation, one can build an emulator based on a limited number of simulation runs and carry out the analysis using the emulator, see e.g. [23, 41, 45, 2]. Among different classes of surrogate models, Gaussian processes (GPs) [34, 36] have gained increasing attention due to their statistical properties such as computational tractability and flexibility. They are flexible models and can fit any smooth, continuous function [29] thanks to the variety of covariance kernels available. Assumptions about the underlying function such as differentiability or periodicity are encoded through kernels. Most importantly, the GP prediction is equipped with an estimation of uncertainty (predictive variance or mean squared error (MSE)) which reflects the quality of the prediction.

GPs are built relying on training data, also called design or sample points, whose locations have a strong effect on the quality of prediction. This has been pointed out by several studies [40, 19]. The design of computer experiments (DoE) refers to selection of the sample locations. DoEs are performed as *one-shot* or *adaptive* [24]: in the former all samples are chosen at once while in the latter points are selected sequentially using information from the emulator and the existing data. A potential drawback of one-shot approaches is that they may result in under/oversampling [39, 9]. However, in adaptive methods we can stop the sampling process, which is computationally expensive, as soon as the emulator achieves an acceptable level of accuracy. Moreover, with adaptive sampling it is possible to take more samples in regions where the underlying function is highly nonlinear or exhibits abrupt changes. It is worth mentioning that the idea of sequential sampling is used in Bayesian optimisation [17, 38] where the goal is to find the global optimum of black-box functions.

This work focuses on GP-based adaptive sampling where an initial design is sequentially extended to improve the prediction performance of the emulator. The initial DoE is often “space-filling” meaning that the points are scattered uniformly over the input space. The most common space-filling designs are: Latin hypercube sampling [27], full factorial [5], minimax and maximin distance [15] and orthogonal array [30]. We refer the reader to [33, 18] and references therein for more information on space-filling designs.

There are many GP-based adaptive sampling methods which can be categorised according to their strategies to choose future sample sites. An intuitive criterion is the predictive

variance embedded in GP modelling. In this framework, the predictive variance is considered as an estimation of the “real” prediction error and the point with a maximum uncertainty is taken as the next experimental design [26, 14]. The predictive variance does not depend directly on the outputs (see Equation (6)) and its magnitude is mainly determined by the location of the points in the input space: MSE grows with distance from data points. As a result, this criterion takes a lot of samples on the boundary which can be a problem if the function’s main characteristics appear inside the interior region. The maximum MSE (MMSE) and integrated MSE (IMSE) are two popular variants of the MSE criterion; the former selects a new point such that the future MMSE is the largest and the latter looks for a sample where the future IMSE is the lowest, see [36, 31]. However, computing MSE and IMSE is cumbersome especially in high dimensions.

The leave-one-out (LOO) cross-validation error gives another class of adaptive sampling criteria, see [22, 21, 1, 25]. To calculate the LOO errors, a GP is first fitted to the training data. Then, one point is removed and the response is predicted at that location. The difference between the predicted response and the true value serves as the LOO error. This procedure is repeated for all the points. A relatively small error indicates that the prediction accuracy in a vicinity of the removed point is high and there is good information about the true function there. On the other hand, a comparably large error means that the removed point has a huge impact on the accuracy of the emulator and hence, we need more samples in the nearby region to reduce the errors. In [42] scores obtained by cross-validation are used to identify regions of distinct model behaviour and specify mixture of covariance functions for GP emulators. Using the LOO errors as sampling criterion has several advantages. First, it provides actual prediction error at the design points. Second, it is model-independent and can be achieved by any surrogate model. For example, in [4] a methodology based on the LOO cross-validation is proposed to estimate the prediction uncertainty of any surrogate model, either deterministic or probabilistic. Third, computing the LOO errors is not expensive in terms of computational cost, see [6]. However, they are not determined everywhere in the input space and only defined at locations where we have pre-existing model runs.

This paper proposes an adaptive sampling approach based on the LOO errors to build GP emulators as accurately as possible for deterministic computer codes over the entire domain. It uses another GP model to estimate the LOO errors at unobserved points. The proposed method has only one parameter to be set and can be easily extended to a batch mode where at each iteration a set of input points is selected for evaluation. This is an important property as it saves the user time when parallel computing is available, see e.g. [43]. The remainder of the paper is organised as follows. In the next section, the statistical methodology of GP emulators is briefly reviewed. Section 3 introduces the proposed adaptive sampling approach and its extension to a batch model. Section 4 deals with numerical experiments where we test the predictive performance of our proposed algorithm. Finally, the paper’s conclusion is in Section 5.

2 Gaussian process models

First we look at GP emulators and their properties. Let the underlying function of a deterministic complex computer code is denoted by $f : \mathcal{D} \mapsto \mathbb{R}$ in which \mathcal{D} is a compact subset in \mathbb{R}^d . Suppose $\mathcal{A} = \{(\mathbf{x}_i, y_i)\}_{i=1}^n$ is a training dataset where $\mathbf{X}_n = (\mathbf{x}_1, \dots, \mathbf{x}_n)^\top$ are n locations in the input space \mathcal{D} with the corresponding outputs (responses/observations) $\mathbf{y}_n = (f(\mathbf{x}_1), \dots, f(\mathbf{x}_n))^\top$. To approximate f , we model \mathbf{y}_n as a Gaussian process $(Z_0(\mathbf{x}))_{\mathbf{x} \in \mathcal{D}}$ whose mean and covariance functions are specified by

$$m_0 : \mathcal{D} \mapsto \mathbb{R} ; m_0(\mathbf{x}) = \mathbb{E}[Z_0(\mathbf{x})] \quad (1)$$

$$k_0 : \mathcal{D} \times \mathcal{D} \mapsto \mathbb{R} ; k_0(\mathbf{x}, \mathbf{x}') = \text{Cov}(Z_0(\mathbf{x}), Z_0(\mathbf{x}')). \quad (2)$$

In this work, $m_0(\mathbf{x})$ is assumed to be a constant function and μ is used to denote the value of this constant which is estimated from the data. The covariance kernel needs to be a positive semi-definite function. The Matérn family of kernels are commonplace in computer experiments and (in the univariate case) are defined as:

$$k_0(x, x') = \sigma^2 \frac{2^{1-\nu}}{\Gamma(\nu)} \left(\frac{\sqrt{2\nu}}{\theta} |x - x'| \right)^\nu B_\nu \left(\frac{\sqrt{2\nu}}{\theta} |x - x'| \right), \quad (3)$$

where $\Gamma(\cdot)$ is the Gamma function and $B_\nu(\cdot)$ denotes the modified Bessel function of the second kind of order ν . The parameter ν determines the degree of smoothness of sample functions; a process with Matérn kernel of order ν is $\lfloor \nu - 1 \rfloor$ times differentiable. The widely-used squared exponential covariance function is a special case of Matérn kernel when $\nu \rightarrow \infty$ and is given by

$$k_0(x, x') = \sigma^2 \exp \left(-\frac{|x - x'|^2}{2\theta^2} \right). \quad (4)$$

The positive parameters σ^2 and θ are referred to as the *process variance* and *correlation length scale*. These parameters are usually unknown and need to be estimated from data. We refer the reader to [34, 10] for an introduction to estimation techniques.

The GP prediction is obtained by conditioning it on the observations:

$$Z_n(\mathbf{x}) = Z_0(\mathbf{x}) \mid \mathbf{y}_n = Z_0(\mathbf{x}) \mid Z_0(\mathbf{x}_1) = f(\mathbf{x}_1), \dots, Z_0(\mathbf{x}_n) = f(\mathbf{x}_n).$$

Given that the unknown parameters are estimated, the conditional mean, $\mathbb{E}[Z_n(\mathbf{x})]$, and covariance, $\text{Cov}(Z_n(\mathbf{x}), Z_n(\mathbf{x}'))$, have closed-form expressions as [34]

$$m_n(\mathbf{x}) = \hat{\mu} + \mathbf{k}(\mathbf{x})^\top \mathbf{K}^{-1}(\mathbf{y}_n - \hat{\mu}\mathbf{1}) \quad (5)$$

$$k_n(\mathbf{x}, \mathbf{x}') = k_0(\mathbf{x}, \mathbf{x}') - \mathbf{k}(\mathbf{x})^\top \mathbf{K}^{-1} \mathbf{k}(\mathbf{x}') + \frac{(1 - \mathbf{1}^\top \mathbf{K}^{-1} \mathbf{k}(\mathbf{x})) (1 - \mathbf{1}^\top \mathbf{K}^{-1} \mathbf{k}(\mathbf{x}'))}{\mathbf{1}^\top \mathbf{K}^{-1} \mathbf{1}}. \quad (6)$$

Here, $\mathbf{k}(\mathbf{x}) = (k_0(\mathbf{x}, \mathbf{x}_1), \dots, k_0(\mathbf{x}, \mathbf{x}_n))^\top$ is the vector of covariances between $Z_0(\mathbf{x})$ and $Z_0(\mathbf{x}_i)$ s and \mathbf{K} is an $n \times n$ covariance matrix with elements $\mathbf{K}_{ij} = k_0(\mathbf{x}_i, \mathbf{x}_j)$, $\forall 1 \leq i, j \leq n$. It is worth mentioning that at a generic location $\mathbf{x}_0 \in \mathcal{D}$, $Z_n(\mathbf{x}_0)$ has a normal distribution characterised by

$$Z_n(\mathbf{x}_0) \sim \mathcal{N}(m_n(\mathbf{x}_0), s_n^2(\mathbf{x}_0)), \quad (7)$$

where $s_n^2(\mathbf{x}_0) = \text{Cov}(Z_n(\mathbf{x}_0), Z_n(\mathbf{x}_0))$ is the conditional variance. It determines the uncertainty associated with the prediction at \mathbf{x}_0 and can be used as a measure of the prediction accuracy. Note that in the Bayesian framework, $m_0(\cdot)$ and $m_n(\cdot)$ are called ‘‘prior’’ and ‘‘posterior’’ mean, respectively as they reflect our beliefs about the underlying function before and after incorporating information from the data points.

3 Proposed adaptive sampling method

An ‘‘efficient’’ adaptive sampling strategy should meet the following conditions [24]:

- (i) **Local exploitation:** that allows us to add more points in interesting areas discovered so far.
- (ii) **Global exploration:** by which unexplored domain regions can be detected.
- (iii) **Trade off between local exploitation and global exploration:** which balances the previous two objectives.

In this work, the proposed adaptive sampling approach uses *expected squared LOO error*, see Section 3.1, for local exploitation; samples are taken in the vicinity of the point whose LOO error is largest. The global exploration and the trade off between the local/global search is driven by the *pseudo expected improvement* criterion introduced in Section 3.2.

3.1 Expected squared LOO cross-validation error

Let $Z_{n,-i}(\mathbf{x})$ is the Gaussian process $Z_0(\mathbf{x})$ conditional on all observations except the i -th one: $Z_{n,-i}(\mathbf{x}) = Z_0(\mathbf{x}) | \mathbf{y}_n \setminus \{f(\mathbf{x}_i)\}$. The predictive mean and variance of $Z_{n,-i}(\mathbf{x})$ are denoted by $m_{n,-i}(\mathbf{x})$ and $s_{n,-i}^2(\mathbf{x})$, respectively. The LOO cross-validation error at the design point \mathbf{x}_i is expressed by

$$e_{LOO}(\mathbf{x}_i) = |m_{n,-i}(\mathbf{x}_i) - f(\mathbf{x}_i)|, \quad (8)$$

which is used as a measure to identify the effect of the i -th data point on the accuracy of the emulator, see e.g. [22, 1]. However, this quantity can be misleading as shown by an example in Figure 1. As can be seen, the LOO error is zero at the fifth sample point, i.e. $(0, 0.5)$, although it plays an important role on the quality of the prediction. The reason is that the LOO error (Equation (8)) only accounts for the difference between the predictive mean and the function value.

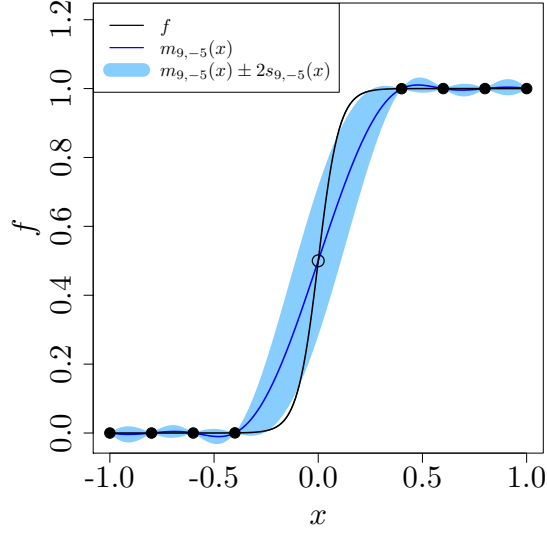


Figure 1: Removing the fifth sample, i.e. $(0, 0.5)$, does not change the prediction at $x = 0$ and the LOO error is zero there: $|m_{9,-5}(x_5) - f(x_5)| = 0$. This means that the sample does not have any influence on the emulator while f has a large gradient there. The true function is $f(x) = \frac{1}{1+\exp(-20x)}$.

In this paper, we use another criterion to measure the sensitivity of the emulator to the left out point. It is called “expected squared LOO error (ESE_{LOO})” whose value at the observed location \mathbf{x}_i is defined as

$$ESE_{LOO}(\mathbf{x}_i) = \frac{\mathbb{E} \left[(Z_{n,-i}(\mathbf{x}_i) - f(\mathbf{x}_i))^2 \right]}{\sqrt{\text{Var} \left((Z_{n,-i}(\mathbf{x}_i) - f(\mathbf{x}_i))^2 \right)}}. \quad (9)$$

In the above equation, both the numerator and denominator, which is used for normalisation, can be expressed in closed-form expressions given by

$$\mathbb{E} \left[(Z_{n,-i}(\mathbf{x}_i) - f(\mathbf{x}_i))^2 \right] = s_{n,-i}^2(\mathbf{x}_i) + (m_{n,-i}(\mathbf{x}_i) - f(\mathbf{x}_i))^2, \quad (10)$$

$$\text{Var} \left((Z_{n,-i}(\mathbf{x}_i) - f(\mathbf{x}_i))^2 \right) = 2s_{n,-i}^4(\mathbf{x}_i) + 4s_{n,-i}^2(\mathbf{x}_i) (m_{n,-i}(\mathbf{x}_i) - f(\mathbf{x}_i))^2. \quad (11)$$

To calculate the closed-form expressions, we note that $Z_{n,-i}(\mathbf{x}_i)$ has a normal distribution (see Figure 2) as follows

$$Z_{n,-i}(\mathbf{x}_i) \sim \mathcal{N} \left(m_{n,-i}(\mathbf{x}_i), s_{n,-i}^2(\mathbf{x}_i) \right). \quad (12)$$

By subtracting $f(\mathbf{x}_i)$ from both sides and dividing them by $s_{n,-i}(\mathbf{x}_i)$, we have

$$\frac{Z_{n,-i}(\mathbf{x}_i) - f(\mathbf{x}_i)}{s_{n,-i}(\mathbf{x}_i)} \sim \mathcal{N}\left(\frac{m_{n,-i}(\mathbf{x}_i) - f(\mathbf{x}_i)}{s_{n,-i}(\mathbf{x}_i)}, 1\right). \quad (13)$$

The square of the left hand side is a random variable with noncentral chi-square distribution

$$\left(\frac{Z_{n,-i}(\mathbf{x}_i) - f(\mathbf{x}_i)}{s_{n,-i}(\mathbf{x}_i)}\right)^2 \sim \chi'^2\left(\kappa = 1, \lambda = \left(\frac{m_{n,-i}(\mathbf{x}_i) - f(\mathbf{x}_i)}{s_{n,-i}(\mathbf{x}_i)}\right)^2\right), \quad (14)$$

where κ and λ are the degrees of freedom and noncentrality parameter, respectively¹. As a result

$$\mathbb{E}\left[\left(\frac{Z_{n,-i}(\mathbf{x}_i) - f(\mathbf{x}_i)}{s_{n,-i}(\mathbf{x}_i)}\right)^2\right] = 1 + \left(\frac{m_{n,-i}(\mathbf{x}_i) - f(\mathbf{x}_i)}{s_{n,-i}(\mathbf{x}_i)}\right)^2, \quad (15)$$

$$\text{Var}\left(\left(\frac{Z_{n,-i}(\mathbf{x}_i) - f(\mathbf{x}_i)}{s_{n,-i}(\mathbf{x}_i)}\right)^2\right) = 2\left(1 + 2\left(\frac{m_{n,-i}(\mathbf{x}_i) - f(\mathbf{x}_i)}{s_{n,-i}(\mathbf{x}_i)}\right)^2\right). \quad (16)$$

Finally, if the expectation and variance in the above equations are multiplied by $s_{n,-i}^2(\mathbf{x}_i)$, we achieve Equations (10) and (11).

The $ESE_{LOO}(\mathbf{x}_i)$ criterion provides more information than the LOO error about the sensitivity of the emulator to the design points. Because $ESE_{LOO}(\mathbf{x}_i)$ accounts for both the prediction uncertainty and the difference between the prediction and the true function at the left out point. In Figure 1, for example, $ESE_{LOO}(x_5)$ is not null contrary to the LOO error. It is notable that we do not re-estimate the unknown parameters for building $Z_{n,-i}(\mathbf{x})$ to alleviate the computational time. Besides, the predictive mean and variance of $Z_{n,-i}(\mathbf{x})$ can be calculated efficiently based on the formula suggested in [6].

The analytical expression of $\mathbb{E}\left[(Z_{n,-i}(\mathbf{x}_i) - f(\mathbf{x}_i))^2\right]$ is similar to the *expected improvement for global fit (EIGF)* infill sampling criterion proposed by Lam [20]. In EIGF, the improvement at an arbitrary point \mathbf{x} is given by:

$$IGF(\mathbf{x}) = (Z_n(\mathbf{x}) - f(\mathbf{x}_i^*))^2, \quad (17)$$

where $f(\mathbf{x}_i^*)$ is the observation at sample point \mathbf{x}_i^* which is closest (in Euclidean distance) to \mathbf{x} . The EIGF criterion is the expected value of $IGF(\mathbf{x})$ that reads

$$EIGF(\mathbf{x}) = \mathbb{E}[IGF(\mathbf{x})] = (m_n(\mathbf{x}) - f(\mathbf{x}_i^*))^2 + s_n^2(\mathbf{x}). \quad (18)$$

Using the above criterion, the next sample is selected where EIGF is maximum: $\mathbf{x}_{n+1} = \underset{\mathbf{x} \in \mathcal{D}}{\text{argmax}} EIGF(\mathbf{x})$. In Section 4, we compare the performance of our method with EIGF on several test functions.

¹Suppose X_1, \dots, X_κ are κ independent random normal variables such that $X_i \sim \mathcal{N}(\mu_i, 1)$, $1 \leq i \leq \kappa$. Then, $\sum_{i=1}^{\kappa} X_i^2 \sim \chi'^2(\kappa, \lambda = \sum_{i=1}^{\kappa} \mu_i^2)$ has a noncentral chi-square distribution with mean $\kappa + \lambda$ and variance $2(\kappa + 2\lambda)$.

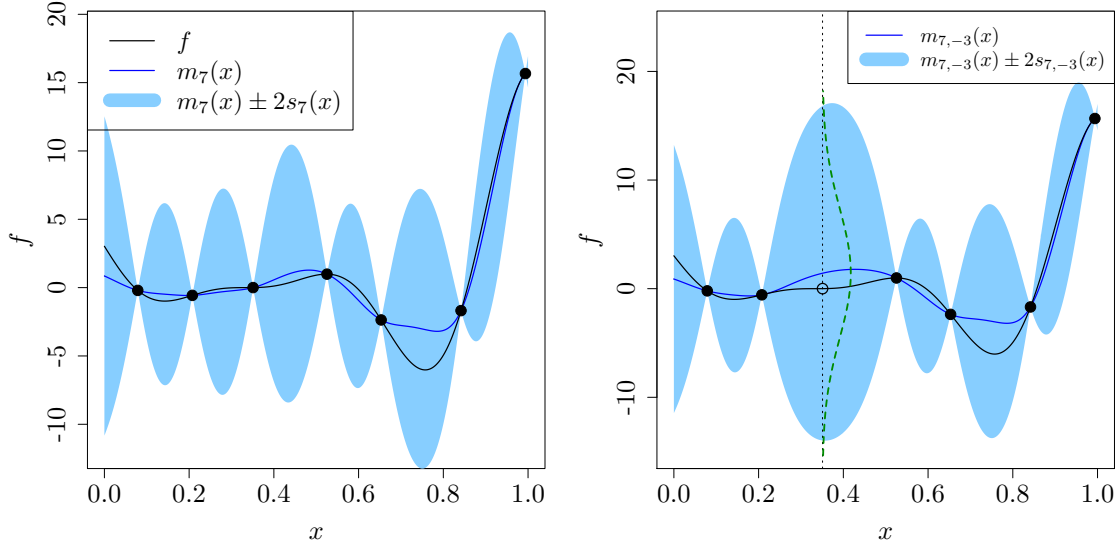


Figure 2: Left: Gaussian process prediction (blue) with 95% credible intervals (shaded) based on 7 observations from the true function (black). Right: GP prediction based on the training data except the third one where the GP has a normal distribution specified by Equation (12).

3.2 Selection criterion

Since the magnitude of $ESE_{LOO}(\mathbf{x}_i)$ at \mathbf{x}_i reflects the sensitivity of the emulator to the loss of information provided by that point, it is reasonable to choose the next sample where $ESE_{LOO}(\mathbf{x})$ is highest. However, this quantity is only defined at the training data, $ESE_{LOO}(\mathbf{x}_i)$, and its maximum value is undetermined. To overcome this problem, one can estimate $ESE_{LOO}(\mathbf{x})$ at unobserved locations using surrogate models. Here, we use another GP model denoted by $Z_n^e(\mathbf{x})$ to approximate $ESE_{LOO}(\mathbf{x})$ and its maximum. The training dataset of $Z_n^e(\mathbf{x})$ is $\{\mathbf{X}_n, \mathbf{y}_n^e\}$ where $\mathbf{y}_n^e = (ESE_{LOO}(\mathbf{x}_1), \dots, ESE_{LOO}(\mathbf{x}_n))^T$.

A naive way to find the maximum of $ESE_{LOO}(\mathbf{x})$ is to maximise the predictive mean of $Z_n^e(\mathbf{x})$. However, this simple strategy does not define a valid optimisation scheme due to *overexploitation* [16] which leads to clustering in a vicinity of the point with the largest $ESE_{LOO}(\mathbf{x}_i)$. To avoid this problem, we maximise an auxiliary function called *pseudo expected improvement (PEI)* (whose idea is introduced in [44]) to choose the next sample:

$$\mathbf{x}_{n+1} = \arg \max_{\mathbf{x} \in \mathcal{D}} PEI(\mathbf{x}). \quad (19)$$

PEI is obtained by multiplying the expected improvement (EI) measure by a repulsive function (RF):

$$PEI(\mathbf{x}) = EI(\mathbf{x})RF(\mathbf{x}), \quad (20)$$

as is visualised in Figure 3.

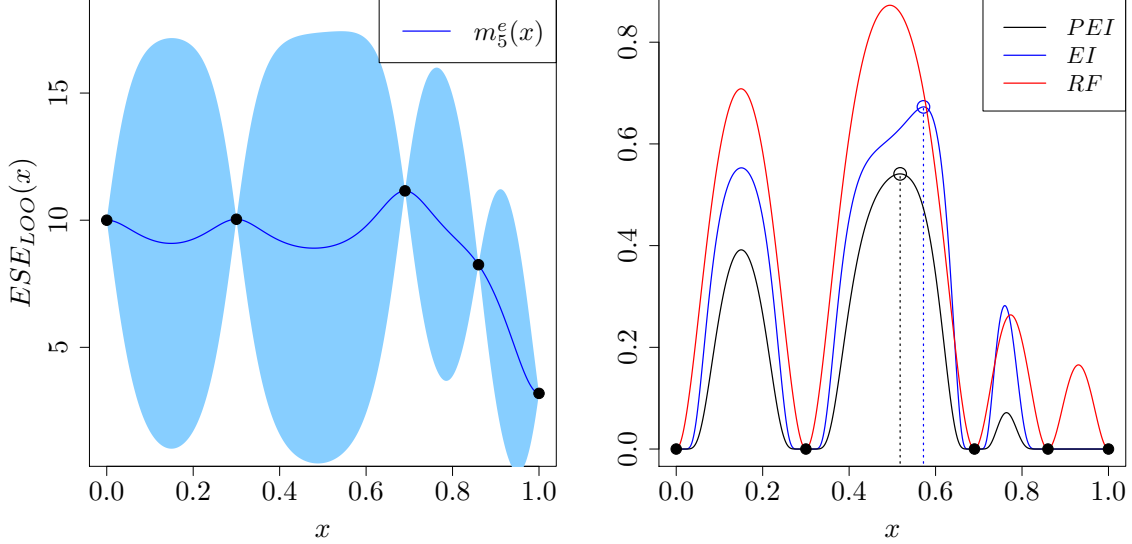


Figure 3: Left: A GP is fitted to five expected squared LOO errors. Right: Pseudo expected improvement (black) is obtained by multiplying expected improvement (blue) by the influence functions (red). The next sample point is where the PEI is maximum (black circle). The maximum of EI is shown by the blue circle. The PEI criterion is more explorative than EI.

EI is a commonplace acquisition function in Bayesian optimisation and is expressed by

$$EI(\mathbf{x}) = \begin{cases} (m_n^e(\mathbf{x}) - \max(\mathbf{y}_n^e)) \Phi(u) + s_n^e(\mathbf{x}) \phi(u) & \text{if } s_n^e(\mathbf{x}) > 0 \\ 0 & \text{if } s_n^e(\mathbf{x}) = 0. \end{cases} \quad (21)$$

Here, $u = \frac{m_n^e(\mathbf{x}) - \max(\mathbf{y}_n^e)}{s_n^e(\mathbf{x})}$, $m_n^e(\mathbf{x})$ and $s_n^e(\mathbf{x})$ are the conditional mean and variance of $Z_n^e(\mathbf{x})$, $\phi(\cdot)$ and $\Phi(\cdot)$ represent the PDF and CDF of the standard normal distribution, respectively. EI is a non-negative, parameter-free function and is null at the data points. It makes a trade off between local/global search during the course of optimisation. However, it is bias towards exploitation, which can be observed from Figure 3, especially at the beginning of the search due to underestimation of the predictive variance, $s_n^e(\mathbf{x})$ [37, 17, 32]. In other words, if EI is used as the select criterion in our method, the next sample point will be close to the point with the highest $ESE_{LOO}(\mathbf{x}_i)$. This is illustrated in Figure 4 where the true function is the Franke’s function, see section 4. In PEI, a repulsive function denoted by $RF(\mathbf{x})$ is multiplied by EI to make it more explorative. $RF(\mathbf{x})$ is a measure of the

(canonical) distance between \mathbf{x} and the data points and defined as

$$RF(\mathbf{x}; \mathbf{X}_n) = \prod_{i=1}^n [1 - \text{Corr}(Z_n^e(\mathbf{x}), Z_n^e(\mathbf{x}_i))], \quad (22)$$

where $\text{Corr}(\cdot, \cdot)$ is the correlation function of $Z_n^e(\cdot)$. The value of $RF(\cdot)$ is between zero and one and is null at the data points because $\text{Corr}(Z_n^e(\mathbf{x}_i), Z_n^e(\mathbf{x}_i)) = 1, \forall \mathbf{x}_i \in \mathbf{X}_n$.

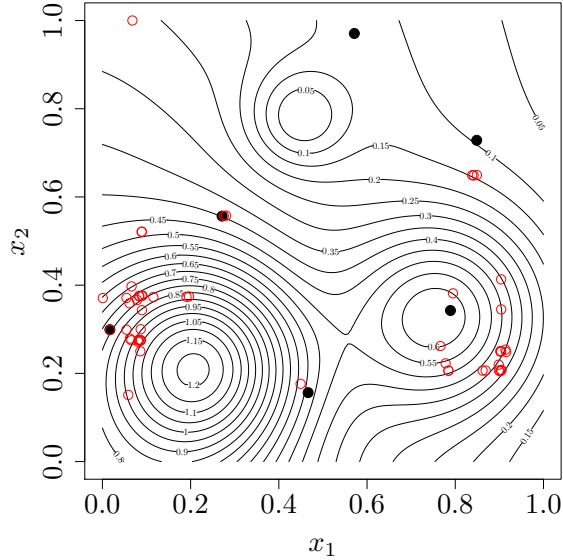


Figure 4: Adaptive designs (red circles) obtained by EI as the selection criterion in the proposed sequential sampling approach. The filled circles are the initial DoE and the true function is Franke’s function, see section 4. EI tends towards exploitation and as a result clustering occurs.

The correlation function $\text{Corr}(\cdot, \cdot)$ depends on length-scales $\boldsymbol{\theta}^e = [\theta_1^e, \dots, \theta_d^e]^\top$ that are estimated from $\{\mathbf{X}_n, \mathbf{y}_n^e\}$. It is important that θ_i^e s do not take very “small” values to circumvent clustering. The reason is that when they come near zero, $\text{Corr}(Z_n^e(\mathbf{x}), Z_n^e(\mathbf{x}_i))$ tends to zero and $RF(\mathbf{x})$ is (almost) one everywhere which means it has no influence on EI. Besides, as $\boldsymbol{\theta}^e \rightarrow 0$ the maximum of EI is located in a shrinking neighbourhood of the current best point [28]. As a result, it is essential to consider a lower bound for $\boldsymbol{\theta}^e$. For a normalised input space, i.e. $\mathcal{D} = [0, 1]^d$, we define this lower bound to be

$$\boldsymbol{\theta}_{lb}^e = \left(\sqrt{-0.5/\ln(10^{-8})}, \dots, \sqrt{-0.5/\ln(10^{-8})} \right)^\top. \quad (23)$$

The lower bound is obtained by setting the minimum correlation to 10^{-8} when the kernel is squared exponential, see Equation (4). The minimum correlation exists between two points with the largest distance from each other which is one in $\mathcal{D} = [0, 1]^d$.

A common issue in adaptive sampling is that many design points lie along the boundary of the input space. Such samples might be nonoptimal if the true model is not feasible on the boundary [11]. This problem can be alleviated by introducing “pseudo points”, denoted by \mathbf{X}_p , at appropriate locations of the design space. Pseudo points are used to update the repulsive function, i.e. $RF(\mathbf{x}; \mathbf{X}_n \cup \mathbf{X}_p)$, but the true function is not evaluated there due to computational cost. In this work, the following locations are considered as the pseudo points

1. corners of the input space ,
2. closest point on each face of the (rectangular) input region to the initial DoE.

For example, the red triangles in Figure 5 are pseudo points in a 2-dimensional space with six initial designs shown by black points. Finally, the steps of the proposed adaptive sampling method are outlined in Algorithm 1.

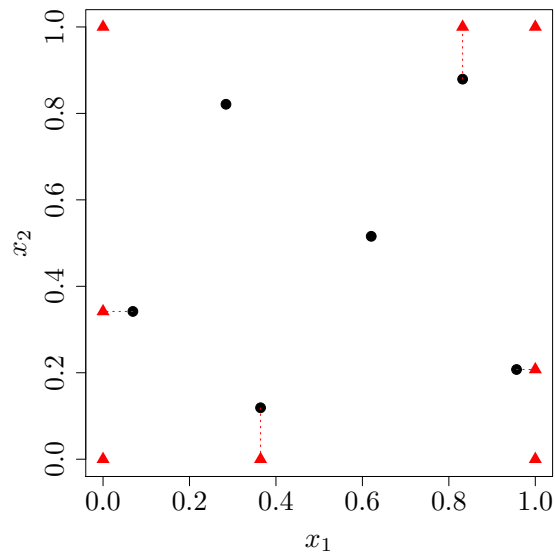


Figure 5: Initial DoE (black points) and pseudo points (red triangles). They are closest point on each face of the input space to the initial DoE and also at the corners of the region.

3.3 Extension to the batch mode

When parallel computing is available, it is preferred to evaluate function f in a set of input points rather than a single point since it saves the user time. In batch sampling at each iteration, $q > 1$ locations denoted by $\mathbf{x}_{n+1}, \dots, \mathbf{x}_{n+q}$ are chosen for evaluation. Note that

Algorithm 1 Proposed sequential sampling approach

- 1: Create an initial design: $\mathbf{X}_n = \{\mathbf{x}_1, \dots, \mathbf{x}_n\}$
 - 2: Evaluate f at \mathbf{X}_n : $\mathbf{y}_n = f(\mathbf{X}_n)$
 - 3: Fit the Gaussian process $Z_n(\mathbf{x})$ to $\{\mathbf{X}_n, \mathbf{y}_n\}$
 - 4: **while not stop do**
 - 5: **for** $i = 1$ to n **do**
 - 6: Calculate $ESE_{LOO}(\mathbf{x}_i)$ using Equation (9)
 - 7: **end for**
 - 8: Set $\mathbf{y}_n^e = (ESE_{LOO}(\mathbf{x}_1), \dots, ESE_{LOO}(\mathbf{x}_n))^\top$
 - 9: Set the lower bound for θ^e using Equation (23)
 - 10: Fit $Z_n^e(\mathbf{x})$ to $\{\mathbf{X}_n, \mathbf{y}_n^e\}$
 - 11: Calculate $PEI(\mathbf{x}) = EI(\mathbf{x})RF(\mathbf{x})$
 - 12: $\mathbf{x}_{n+1} \leftarrow \operatorname{argmax} PEI(\mathbf{x})$ and set $\mathbf{X}_n = \mathbf{X}_n \cup \{\mathbf{x}_{n+1}\}$
 - 13: $y_{n+1} \leftarrow f(\mathbf{x}_{n+1})$ and set $\mathbf{y}_n = \mathbf{y}_n \cup \{y_{n+1}\}$
 - 14: Update $Z_n(\mathbf{x})$ using the new data point $(\mathbf{x}_{n+1}, y_{n+1})$
 - 15: $n \leftarrow n + 1$
 - 16: **end while**
-

the computation time of running the simulator on q parallel cores is the same as a single run. We show that the PEI criterion is eligible to be used in a batch mode thanks to the repulsive function. Suppose \mathbf{x}_{n+1} is obtained by maximising the PEI criterion. The next sample location, i.e. \mathbf{x}_{n+2} , is where the updated PEI is maximum. To update PEI, the initial EI is multiplied by $RF(\mathbf{x}; \mathbf{X}_n \cup \mathbf{x}_{n+1})$ which is defined as

$$RF(\mathbf{x}; \mathbf{X}_n \cup \mathbf{x}_{n+1}) = \prod_{i=1}^{n+1} [1 - \operatorname{Corr}(Z_n^e(\mathbf{x}), Z_n^e(\mathbf{x}_i))]. \quad (24)$$

Notice that RF does not depend on the function values and \mathbf{x}_{n+2} is obtained without evaluating f at \mathbf{x}_{n+1} . By repeating the previous steps, all the q locations are selected

$$RF(\mathbf{x}; \mathbf{X}_n \cup \mathbf{x}_{n+1} \cup \dots \cup \mathbf{x}_{n+q-1}) = \prod_{i=1}^{n+q-1} [1 - \operatorname{Corr}(Z_n^e(\mathbf{x}), Z_n^e(\mathbf{x}_i))]$$
$$\mathbf{x}_{n+q} = \operatorname{argmax}_{\mathbf{x} \in \mathcal{D}} EI(\mathbf{x}) RF(\mathbf{x}; \mathbf{X}_n \cup \mathbf{x}_{n+1} \cup \dots \cup \mathbf{x}_{n+q-1}).$$

An example is illustrated in Figure 6 where $q = 3$ points are selected in one iteration.

4 Numerical experiments

Experimental results are presented and discussed in this section. Four analytic test functions and two real-world problems are considered as the “true” function to assess the effi-

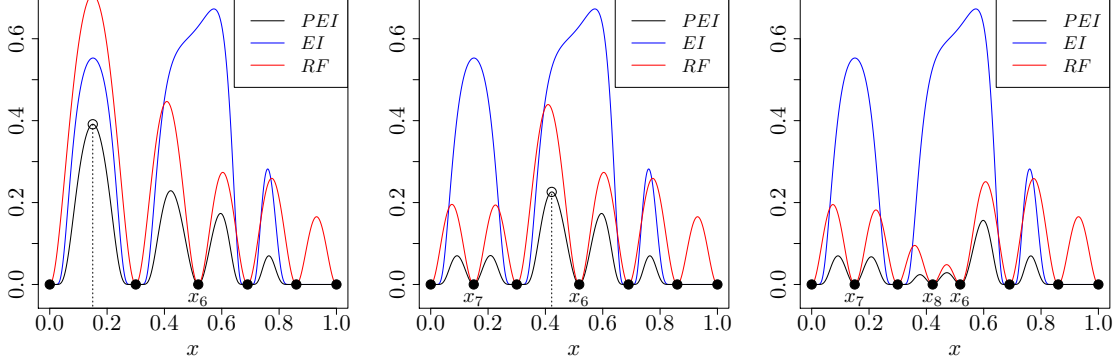


Figure 6: The process of selecting a batch of $q = 3$ points, x_{n+j} , $1 \leq j \leq 3$, where the size of initial DoE is $n = 5$. Left: the first query point, x_6 , is chosen where PEI is maximum. Middle: PEI is updated by multiplying the initial EI by $RF(x; x_{1:5} \cup x_6)$. The second query point, x_7 , is the location of maximum updated PEI. Right: PEI is updated using x_7 and the third sample, x_8 , is selected as explained.

ciency of our proposed sampling method. The results are compared with other approaches including MSE, EIGF [20] and one-shot Latin hypercube sampling (LHS).

4.1 Experimental setup

The prediction accuracy is assessed by the *root mean squared error (RMSE)* criterion which measures the distance between the emulator and the true function. Let $\{(\mathbf{x}_t, f(\mathbf{x}_t))\}_{t=1}^{t=N}$ be a set of N test points. RMSE is defined as

$$RMSE = \sqrt{\frac{\sum_{t=1}^N (m_n(\mathbf{x}_t) - f(\mathbf{x}_t))^2}{N}}, \quad (25)$$

where $m_n(\mathbf{x}_t)$ is the GP prediction at a test site \mathbf{x}_t . The test set has a size $N = 3000$ and its elements are selected uniformly across the input space. A total budget equal to $30d$ is considered for each experiment. The initial space-filling DoE is of size $3d$ and is obtained using the `maximinESE_LHS` function implemented in the R package `DiceDesign` [7]. There are ten different initial DoEs for every function and we assess the prediction performance of each method using all ten sets. The R package `DiceKriging` [35] is employed to construct GP models. The covariance kernel for modelling the true function and ESE_{LOO} is Matérn with $\nu = 3/2$. Since ESE_{LOO} is a positive quantity, its natural logarithm, i.e. $\ln(ESE_{LOO})$, is used when fitting the GP.

4.2 Test functions

The four test functions are

- $f_1(\mathbf{x})$: Franke’s function [12], $d = 2$
- $f_2(\mathbf{x})$: Hartman function [13], $d = 3$
- $f_3(\mathbf{x})$: Friedman function [8], $d = 5$
- $f_4(\mathbf{x})$: Gramacy & Lee function [11], $d = 6$

The analytic expression of the above functions are given in Appendix A. Figure 7 illustrates the prediction performance of our proposed method ESE_{LOO} : sequential (black) and batch with $q = 4$ (orange), MSE (blue) and EIGF (red). Each curve represents the median of ten RMSEs using ten different initial DoEs. The x -axis shows the number of function evaluations divided by the problem dimension, d . The y -axis is on logarithmic scale. The dashed grey lines are the median of RMSEs based on one-shot LHS of sizes (from top to bottom): $10d$, $20d$ and $30d$, respectively.

Generally, the prediction performance of our method is comparable to other approaches. In particular, it outperforms MSE and EIGF in approximating the Hartman (f_2) and Gramacy & Lee (f_4) functions. The sequential (black) and batch (orange) ESE_{LOO} have similar performances; their RMSEs are monotonically (almost linearly) decreasing. This is not the case of MSE and EIGF. The MSE method does not perform well in dimensions 5 and 6. It seems that MSE selects many samples on the boundary of the input space where the GP predictive variance is high. The EIGF method has the best performance only on the Friedman function (f_3) and has the lowest accuracy in approximating other functions, especially f_4 .

4.3 Real-world problems

We also tested our method on two real-world problems which are the 6-dimensional *output transformerless (OTL) circuit* and 7-dimensional *piston simulation* functions [3]. The former (f_{OTL}) returns the midpoint voltage of a transformerless circuit and the latter (f_{piston}) measures the cycle time that a piston takes to complete one cycle within a cylinder. The analytical expressions of f_{OTL} and f_{piston} and their design spaces are given in Appendix B. Figure 8 illustrates the results of comparing our proposed method with MSE, EIGF and LHS design. The experimental setup is the same as explained in Section 4.1. The sequential (black) and batch (orange) ESE_{LOO} have again similar performances and are the best sampling approaches on the piston simulation function. The RMSE criterion associated with ESE_{LOO} (both sequential and batch) reduces steadily on the two problems as is observed in Figure 7. The MSE approach does not work well especially after almost $10 \times d$ function evaluations. It seems that MSE is not a good sampling strategy when the dimensionality of the problem is larger than 5. While EIGF has the best performance on the OTL circuit problem, there is no improvement in the prediction accuracy of the emulator after $10 \times d$ evaluations of the piston simulation function.

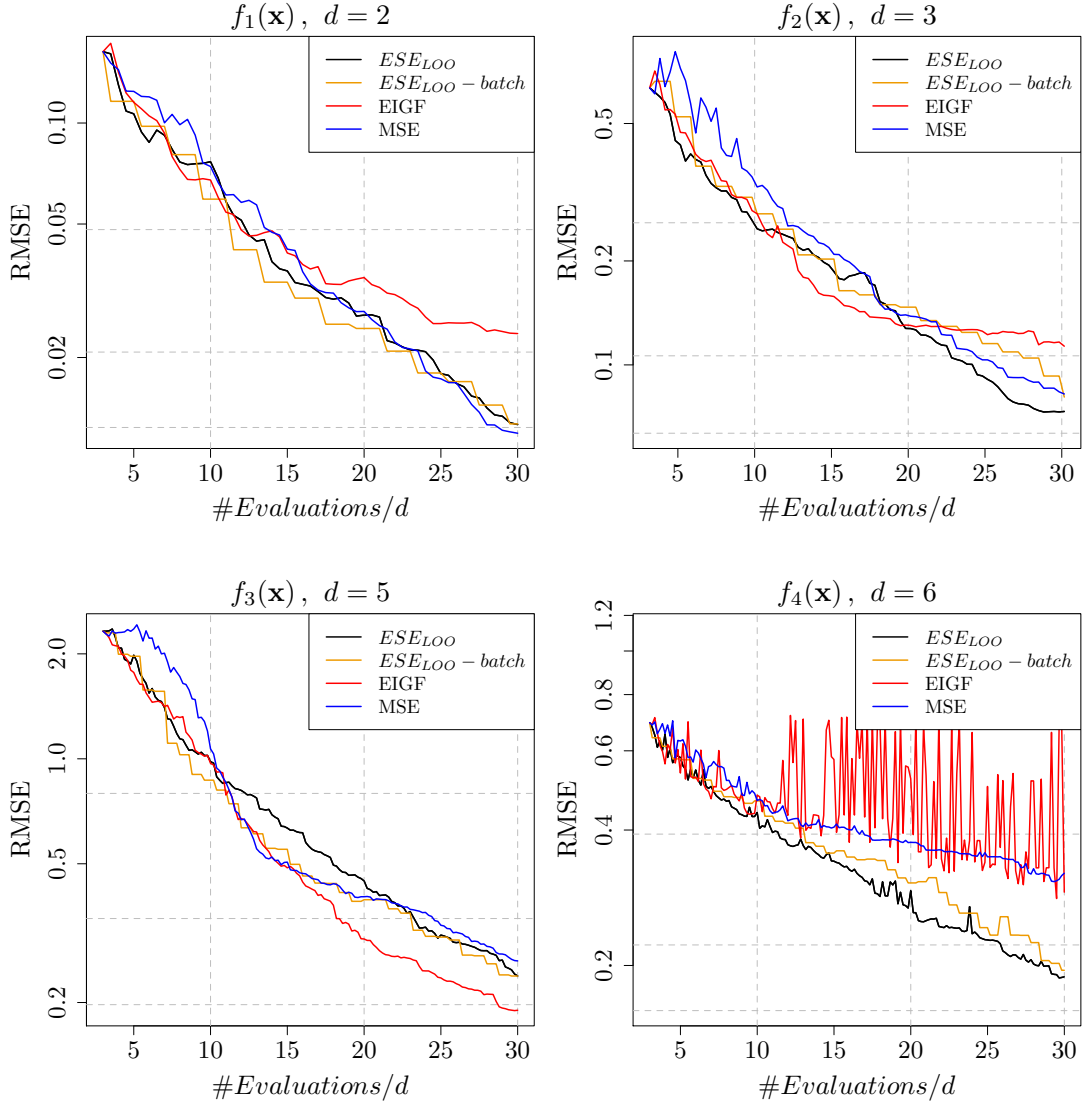


Figure 7: The median of ten RMSEs of our proposed approach ESE_{LOO} : sequential (black) and batch with $q = 4$ (orange), EIGF (red) and MSE (blue). Ten different initial DoEs of size $3d$ are considered for each function; every method produces ten predictions based on them. The total budget is $30d$. The dashed grey lines show the median of RMSEs based on one-shot space-filling designs of sizes (from top to bottom): $10d$, $20d$ and $30d$, respectively. The y -axis is on logarithmic scale.

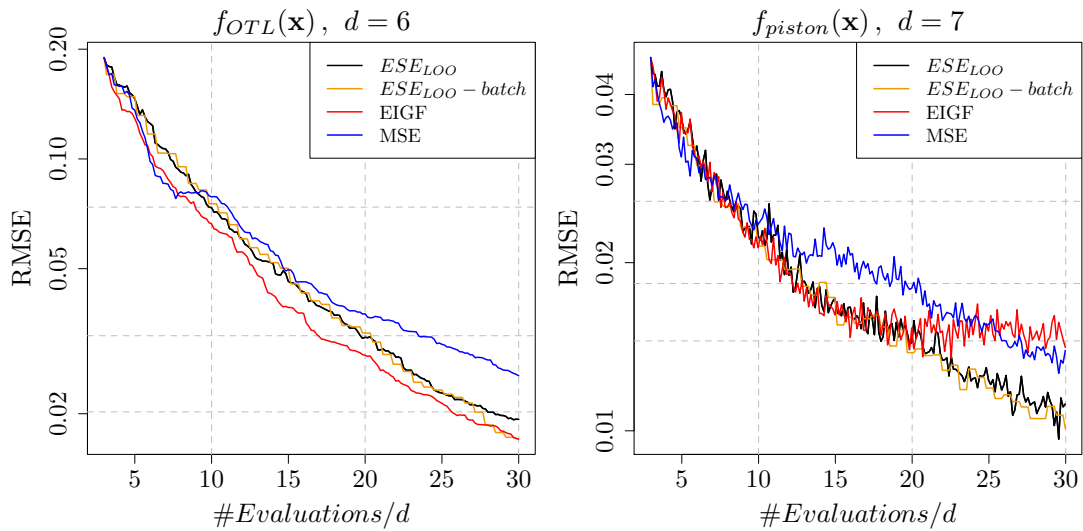


Figure 8: The median of ten RMSEs of our proposed approach ESE_{LOO} : sequential (black) and batch with $q = 4$ (orange), EIGF (red) and MSE (blue). The dashed grey lines show the median of RMSEs based on one-shot space-filling designs of sizes (from top to bottom): $10d, 20d$ and $30d$, respectively.

5 Conclusion

This paper deals with the problem of extending an initial experiment sequentially for training GP models. This is an important issue in the context of emulating computationally expensive computer codes where the goal is to approximate the underlying function with a minimum number of evaluation. An adaptive sampling scheme is presented based on the expected squared leave-one-out error, ESE_{LOO} , which is used to identify “good” locations for future function evaluations. Since ESE_{LOO} is only known at the design points, another GP model is applied to approximate it at unobserved sites. Then, the pseudo expected improvement criterion is employed to find the location of maximum of ESE_{LOO} as the most promising point to improve the emulator. Once the new sample is chosen, it is added to the existing designs and the procedure is repeated until a stopping criterion is met. The proposed method can be easily promoted to a batch mode where at each iteration a set of input points is selected for evaluation. This can save the user time if parallel computing is available. Several test functions are used to test the capability of our method and it is compared with two other methods relying on the mean squared error and expected improvement for global fit criteria. The results show that the proposed adaptive sampling approach is promising.

Acknowledgements

The authors gratefully acknowledge the financial support of the EPSRC via grant EP/N014391/1.

Appendix A Test function expressions

The analytic expressions of four test functions used in our experiments are given below.

1. $f_1(\mathbf{x}) = 0.75 \exp\left(-\frac{(9x_1-2)^2}{4} - \frac{(9x_2-2)^2}{4}\right) + 0.75 \exp\left(-\frac{(9x_1+1)^2}{49} - \frac{9x_2+1}{10}\right) + 0.5 \exp\left(-\frac{(9x_1-7)^2}{4} - \frac{(9x_2-3)^2}{4}\right) - 0.2 \exp(-(9x_1-4)^2 - (9x_2-7)^2).$

2. $f_2(\mathbf{x}) = -\sum_{i=1}^4 \alpha_i \exp\left(\sum_{j=1}^3 \mathbf{A}_{ij} (x_j - \mathbf{P}_{ij})^2\right)$ where $\alpha = (1, 1.2, 3, 3.2)^\top$,

$$\mathbf{A} = \begin{bmatrix} 3 & 10 & 30 \\ 0.1 & 10 & 35 \\ 3 & 10 & 30 \\ 0.1 & 10 & 35 \end{bmatrix}, \quad \mathbf{P} = 10^{-4} \begin{bmatrix} 3689 & 1170 & 2673 \\ 4699 & 4387 & 7470 \\ 1091 & 8732 & 5547 \\ 381 & 5743 & 8828 \end{bmatrix}.$$

3. $f_3(\mathbf{x}) = 10 \sin(\pi x_1 x_2) + 20(x_3 - 0.5)^2 + 10x_4 + 5x_5.$

4. $f_4(\mathbf{x}) = \exp(\sin([0.9(x_1 + 0.48)]^{10})) + x_2 x_3 + x_4.$

Appendix B Real-world function expressions

OTL circuit function The function f_{OTL} is defined as

$$f_{OTL}(\mathbf{x}) = \frac{(V_{b1} + 0.74)\beta(R_{c2} + 9)}{\beta(R_{c2} + 9) + R_f} + \frac{11.35R_f}{\beta(R_{c2} + 9) + R_f} + \frac{0.74R_f\beta(R_{c2} + 9)}{(\beta(R_{c2} + 9) + R_f)R_{c1}},$$

where $V_{b1} = \frac{12R_{b2}}{R_{b1} + R_{b2}}$. The input variables of f_{OTL} are:

- $R_{b1} \in [50, 150]$ is the resistance b_1 (K-Ohms)
- $R_{b2} \in [25, 70]$ is the resistance b_2 (K-Ohms)
- $R_f \in [0.5, 3]$ is the resistance f (K-Ohms)
- $R_{c1} \in [1.2, 2.5]$ is the resistance c_1 (K-Ohms)
- $R_{c2} \in [0.25, 1.2]$ is the resistance c_2 (K-Ohms)
- $\beta \in [50, 300]$ is the current gain c_1 (Amperes).

Piston simulation function The function f_{piston} is defined as

$$f_{piston}(\mathbf{x}) = 2\pi \sqrt{\frac{M}{k + S^2 \frac{P_0 V_0 T_a}{T_0 V^2}}}, \quad \text{where } V = \frac{S}{2k} \left(\sqrt{A^2 + 4k \frac{P_0 V_0}{T_0} T_a} - A \right),$$

$$A = P_0 S + 19.62M - \frac{kV_0}{S}.$$

The input variables of f_{piston} are:

- $M \in [30, 60]$ is the piston weight (kg)
- $S \in [0.005, 0.020]$ is the piston surface area (m^2)
- $V_0 \in [0.002, 0.010]$ is the initial gas volume (m^3)
- $k \in [1000, 5000]$ is the spring coefficient (N/m)
- $P_0 \in [90000, 110000]$ is the atmospheric pressure (N/m^2)
- $T_a \in [290, 296]$ is the ambient temperature (K)
- $T_0 \in [340, 360]$ is the filling gas temperature (K).

References

- [1] V. Aute, K. Saleh, O. Abdelaziz, S. Azarm, and R. Radermacher. Cross-validation based single response adaptive design of experiments for kriging metamodeling of deterministic computer simulations. *Structural and Multidisciplinary Optimization*, 48(3):581–605, 2013.
- [2] Gregory A. Banyay, Michael D. Shields, and John C. Brigham. Efficient global sensitivity analysis for flow-induced vibration of a nuclear reactor assembly using kriging surrogates. *Nuclear Engineering and Design*, 341:1 – 15, 2019.
- [3] Einat Neumann Ben-Ari and David M. Steinberg. Modeling data from computer experiments: An empirical comparison of kriging with mars and projection pursuit regression. *Quality Engineering*, 19(4):327–338, 2007.
- [4] M. Ben Salem, O. Roustant, F. Gamboa, and L. Tomaso. Universal prediction distribution for surrogate models. *SIAM/ASA Journal on Uncertainty Quantification*, 5(1):1086–1109, 2017.
- [5] G. E. P. Box and J. S. Hunter. The 2^{k-p} fractional factorial designs part ii. *Technometrics*, 3(4):449–458, 1961.
- [6] Olivier Dubrule. Cross validation of kriging in a unique neighborhood. *Journal of the International Association for Mathematical Geology*, 15(6):687–699, 1983.
- [7] Delphine Dupuy, Céline Helbert, and Jessica Franco. DiceDesign and DiceEval: two R packages for design and analysis of computer experiments. *Journal of Statistical Software*, 65(11):1–38, 2015.
- [8] Jerome H. Friedman. Multivariate adaptive regression splines. *The Annals of Statistics*, 19(1):1–67, 1991.
- [9] Sushant S. Garud, Iftekhar A. Karimi, and Markus Kraft. Design of computer experiments: A review. *Computers & Chemical Engineering*, 106:71 – 95, 2017. ESCAPE-26.
- [10] Andrew Gelman, John Carlin, Hal Stern, David Dunson, Aki Vehtari, and Donald Rubin. Bayesian Data Analysis, Third Edition (Chapman & Hall/CRC Texts in Statistical Science). Hardcover, 2013.
- [11] Robert B. Gramacy and Herbert K. H. Lee. Adaptive design and analysis of super-computer experiments. *Technometrics*, 51(2):130–145, 2009.
- [12] Ben Haaland and Peter Z. G. Qian. Accurate emulators for large-scale computer experiments. *The Annals of Statistics*, 39(6):2974–3002, 2011.

- [13] Momin Jamil and Xin-She Yang. A literature survey of benchmark functions for global optimization problems. *International Journal of Mathematical Modelling and Numerical Optimisation*, 4(2):150–194, 2013.
- [14] Ruichen Jin, Wei Chen, and Agus Sudjianto. On sequential sampling for global meta-modeling in engineering design. In *Design Engineering Technical Conferences And Computers and Information in Engineering*, volume 2, pages 539–548, 2002.
- [15] M.E. Johnson, L.M. Moore, and D. Ylvisaker. Minimax and maximin distance designs. *Journal of Statistical Planning and Inference*, 26(2):131 – 148, 1990.
- [16] Donald R. Jones. A taxonomy of global optimization methods based on response surfaces. *Journal of Global Optimization*, 21(4):345–383, Dec 2001.
- [17] Donald R. Jones, Matthias Schonlau, and William J. Welch. Efficient global optimization of expensive black-box functions. *Journal of Global Optimization*, 13(4):455–492, 1998.
- [18] V. Roshan Joseph. Space-filling designs for computer experiments: A review. *Quality Engineering*, 28(1):28–35, 2016.
- [19] Crombecq Karel, Dirk Gorissen, Dirk Deschrijver, and Tom Dhaene. A novel hybrid sequential design strategy for global surrogate modeling of computer experiments. *SIAM Journal on Scientific Computing*, 33(4):1948–1974, 2011.
- [20] Chen Quin Lam. *Sequential adaptive designs in computer experiments for response surface model fit*. PhD thesis, Columbus, OH, USA, 2008. AAI3321369.
- [21] Loic Le Gratiet and Claire Cannamela. Kriging-based sequential design strategies using fast cross-validation techniques with extensions to multi-fidelity computer codes. *arXiv e-prints*, page arXiv:1210.6187, 2012.
- [22] Genzi Li, Vikrant Aute, and Shapour Azarm. An accumulative error based adaptive design of experiments for offline metamodeling. *Structural and Multidisciplinary Optimization*, 40(1):137–157, 2009.
- [23] D. Liu, A. Litvinenko, C. Schillings, and V. Schulz. Quantification of airfoil geometry-induced aerodynamic uncertainties—comparison of approaches. *SIAM/ASA Journal on Uncertainty Quantification*, 5(1):334–352, 2017.
- [24] Haitao Liu, Yew-Soon Ong, and Jianfei Cai. A survey of adaptive sampling for global metamodeling in support of simulation-based complex engineering design. *Structural and Multidisciplinary Optimization*, 57(1):393–416, 2018.

- [25] Haitao Liu, Shengli Xu, Ying Ma, Xudong Chen, and Xiaofang Wang. An adaptive Bayesian sequential sampling approach for global metamodeling. *Journal of Mechanical Design*, 138(1), 2015.
- [26] Jay Martin and Timothy Simpson. Use of adaptive metamodeling for design optimization. In *9th AIAA/ISSMO Symposium on Multidisciplinary Analysis and Optimization*, pages 1–9, 2002.
- [27] M. D. McKay, R. J. Beckman, and W. J. Conover. A comparison of three methods for selecting values of input variables in the analysis of output from a computer code. *Technometrics*, 21(2):239–245, 1979.
- [28] Hossein Mohammadi. *Kriging-based black-box global optimization: analysis and new algorithms*. PhD thesis, École Nationale Supérieure des Mines de Saint-Étienne, France, 2016.
- [29] Radford M. Neal. Regression and classification using Gaussian process priors. pages 475–501. *Bayesian Statistics 6*, Oxford University Press, 1998.
- [30] Art B. Owen. Orthogonal arrays for computer experiments, integration and visualization. *Statistica Sinica*, 2(2):439–452, 1992.
- [31] V. Picheny, D. Ginsbourger, O. Roustant, R. T. Haftka, and N. H. Kim. Adaptive designs of experiments for accurate approximation of a target region. *Journal of Mechanical Design*, 132(7):1–9, 2010.
- [32] W. Ponweiser, T. Wagner, and M. Vincze. Clustered multiple generalized expected improvement: A novel infill sampling criterion for surrogate models. In *2008 IEEE Congress on Evolutionary Computation (IEEE World Congress on Computational Intelligence)*, pages 3515–3522, 2008.
- [33] Luc Pronzato and Werner G. Müller. Design of computer experiments: space filling and beyond. *Statistics and Computing*, 22(3):681–701, 2012.
- [34] Carl Edward Rasmussen and Christopher K. I. Williams. *Gaussian processes for machine learning (adaptive computation and machine learning)*. The MIT Press, 2005.
- [35] Olivier Roustant, David Ginsbourger, and Yves Deville. DiceKriging, DiceOptim: Two R packages for the analysis of computer experiments by kriging-based metamodeling and optimization. *Journal of Statistical Software*, 51(1):1–55, 2012.
- [36] Jerome Sacks, William J. Welch, Toby J. Mitchell, and Henry P. Wynn. Design and analysis of computer experiments. *Statistical Science*, 4(4):409–423, 1989.
- [37] Matthias Schonlau. *Computer experiments and global optimization*. PhD thesis, University of Waterloo, 1997.

- [38] B. Shahriari, K. Swersky, Z. Wang, R. P. Adams, and N. de Freitas. Taking the human out of the loop: a review of Bayesian optimization. *Proceedings of the IEEE*, 104(1):148–175, 2016.
- [39] Razi Sheikholeslami and Saman Razavi. Progressive latin hypercube sampling: an efficient approach for robust sampling-based analysis of environmental models. *Environmental Modelling & Software*, 93:109 – 126, 2017.
- [40] T.W. Simpson, J.D. Poplinski, P. N. Koch, and J.K. Allen. Metamodels for computer-based engineering design: Survey and recommendations. *Engineering with Computers*, 17(2):129–150, 2001.
- [41] Ian Vernon, Junli Liu, Michael Goldstein, James Rowe, Jen Topping, and Keith Lindsey. Bayesian uncertainty analysis for complex systems biology models: emulation, global parameter searches and evaluation of gene functions. *BMC Systems Biology*, 12(1):1, 2018.
- [42] Victoria Volodina and Daniel Williamson. Diagnostics-driven nonstationary emulators using kernel mixtures. *SIAM/ASA Journal on Uncertainty Quantification*, 8(1):1–26, 2020.
- [43] Daniel Williamson. Exploratory ensemble designs for environmental models using k-extended Latin Hypercubes. *Environmetrics*, 26(4):268–283, 2015.
- [44] Dawei Zhan, Jiachang Qian, and Yuansheng Cheng. Pseudo expected improvement criterion for parallel EGO algorithm. *Journal of Global Optimization*, 68(3):641–662, 2017.
- [45] Yiming Zhang, Nam H. Kim, Chanyoung Park, and Raphael T. Haftka. Multifidelity surrogate based on single linear regression. *AIAA Journal*, 56(12):4944–4952, 2018.